Solar and Stellar Flares and their Effects on Planets
Proceedings IAU Symposium No. 320, 2015
A.G. Kosovichev, S.L. Hawley & P. Heinzel, eds.

doi:10.1017/S1743921316000557

Searching for failed eruptions interacting with overlying magnetic field

Dominik Gronkiewicz[1,2], **Tomasz Mrozek**[2,3], **Sylwester Kołomański**[2] **and Martyna Chruślińska**[4]

[1]Nicolaus Copernicus Astronomical Center, Polish Academy of Sciences, ul. Bartycka 18, 00-716 Warsaw, Poland email: gronki@camk.edu.pl

[2]Astronomical Institute, University of Wrocław, ul. Kopernika 11, 51-622 Wrocław, Poland

[3]Space Research Centre, PAS, ul. Kopernika 11, 51-622 Wrocław, Poland

[4]Astronomical Observatory, University of Warsaw, Al. Ujazdowskie 4, 00-478 Warsaw, Poland

Abstract. It is well known that not all solar flares are connected with eruptions followed by coronal mass ejection (CME). Even strongest X-class flares may not be accompanied by eruptions or are accompanied by failed eruptions. One of important factor that prevent eruption from developing into CME is strength of the magnetic field overlying flare site. Few observations show that active regions with specific magnetic configuration may produce many CME-less solar flares. Therefore, forecasts of geoeffective events based on active region properties have to take into account probability of confining solar eruptions. Present observations of SDO/AIA give a chance for deep statistical analysis of properties of an active region which may lead to confining an eruption. We developed automated method which can recognize eruptions in AIA images. With this tool we will be able to analyze statistical properties of failed eruptions observed by AIA telescope.

Keywords. Sun: corona, Sun: atmospheric motions, methods: data analysis, techniques: image processing

1. Introduction

According to Gilbert *et al.* (2007), on the basis of kinematic criteria, solar coronal eruptions may be grouped into three classes described in Table 1. In this work we concentrated on the 3rd class, the eruptions which, after initial acceleration in low corona, decelerate and stop eventually due to various mechanism:

- Insufficient energy to escape the gravitational potential of the Sun.
- Properties of overlying magnetic field. (Torök & Kliem 2005; Wang & Zhang 2007)
- Magnetic tension within the erupting flux rope (Vršnak 1990)
- Momentum exchange with the background plasma (Archontis & Török 2008)
- Kink instability and stabilization of the erupting filament (Torök & Kliem 2005; Ji *et al.* 2003)
- Reconnection with the overlying field arcade (Amari *et al.* 1999)

Major observational characteristics of failed eruptions are as follow:

- Untwisting motion of erupting flux ropes (Ji *et al.* 2003)
- Brightenings in footpoints of overlying loops as a result of electron acceleration (Netzel *et al.* 2012)
- Heating of overlying loops (Song *et al.* 2014)
- Visible interaction betweeen the eruption and overlying loops (Mrozek 20011)
- Radio emission in deceleration region (Kushwaha *et al.* 2015)

Table 1. Classification of solar eruptions.

Type	Ejected
Full	> 90% of matter and magnetic structure
Partial(a)	Entire magnetic structure, part of matter
Partial(b)	Part of magnetic structure, small part of matter
Failed	Neither matter nor magnetic structure

In space weather predictions failed eruptions are usually omitted as events which not lead to geoeffective storms. However, detailed statistical analysis of failed eruptions will provide more precise boundary conditions for full eruption occurence from active region of given physical condition. With present, huge observational data base from Solar Dynamics Observatory we are able to search and catalogue failed eruptions in more systematic way. In this paper we describe an algorithm that we use to search for dynamic events in SDO data base.

2. Algorithm description

With our method, SDO/AIA 171 Å synoptic data series (1024x1024 full-disk images) were chosen for analysis. Downloading and processing data is performed automatically. A standard tool used for motion detection is running difference of two consecutive frames. We introduced a slight modification to this technique that is very efficient in extraction of faint, fast-moving objects. Before differentiation simple transformation is applied to the image in following way (where I denotes the intensity of pixel (x, y) at time t and α is a constant): $J(x, y, t) = \ln(I(x, y, t) + \alpha)$. We have found that this technique is far more efficient for moving structures recognition, and it helps to eliminate stationary loops and most of flares in the very preliminary phase of image analysis. Behaviour of each pixel can be described by its state $\hat{S} = (I, V)$ where

$$V = \sqrt{\left(\frac{dJ}{dt}\right)^2 + \frac{1}{4}\left(\frac{d^2J}{dt^2}\right)^2} \ .$$

The next step is to classify state $\hat{S}$ of each pixel to one of the classes: class E (eruption) for areas containing the eruption and Q (quiet) describing the remaining part of the image. We use probabilistic approach. We select 20% of frames with lowest values of squared derivatives (marked with boxes in Figure 1, panel a) and assume that all pixels in these frames belong to class Q. Histogram of (I, V) pairs for these frames, which yields the distribution $P(\hat{S}|Q)$, is presented in Figure 1 (panel b). Similar histogram is made for all frames (Figure 1, panel c) in order to provide $P(\hat{S})$. A priori probability $P(E|\hat{S})$ can be then computed iteratively using Bayes theorem:

$$P\left(E|\hat{S}\right) = 1 - P(Q)\frac{P\left(\hat{S}|Q\right)}{P(\hat{S})} \quad \text{where} \quad P(Q) = 1 - \frac{area_{eruptions}}{area_{total}}$$

3. Results and Discussion

Three months of observations between 01-Apr-2012 and 01-Jul-2012 were analyzed. Automatic algorithm has found 618 events. They were manually browsed and categorized into six classes.

https://doi.org/10.1017/S1743921316000557 Published online by Cambridge University Press

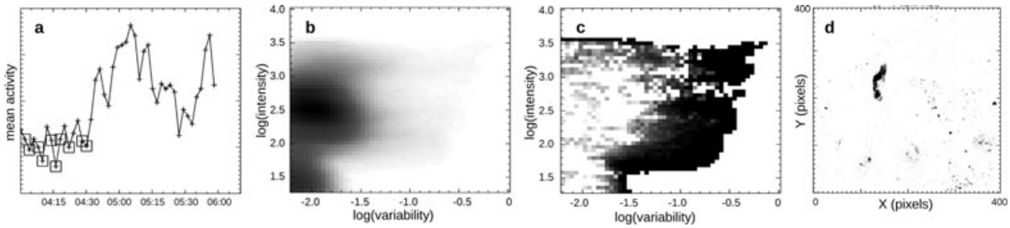

Figure 1. (a) Mean values of squared derivatives for each frame; squares mark frames chosen as quiet Sun reference; (b) Histogram of intensity and variability for each pixel; (c) A priori probability; dark area are eruption pixels; (d) Probability re-mapped to the image. Eruption as well as some smaller fluctuations have been detected.

About 26% of found events were solar eruptions, 70% of which were failed eruptions. There was also large contribution from surges – almost 18%. Relative large number of errors (18%) was caused by dark frames which were unfiltered from sequences. The largest group of uncategorized phenomena (35%) included prominence plasma motions, large-scale loop motions or other events.

The results were compared to events obtained from HEK database (Hurlburt 2012), containing eruptions found by Eruption Patrol algorithm described by Hurlburt (2015). The 200 events were present in analyzed time range, which is slightly less than our results (270). The overall spatial distribution of events is in general agreement with our method.

Presented method is moderately effective in searching for eruption candidates in large datasets, allowing real-time processing. Apart from eruptions, it is extremely sensitive to motions of faint plasma structures high in the corona, including expansion, untwisting, oscillations and EIT waves. Such events could be easily missed during manual browsing of SDO/AIA data. However, the output catalog is uncertain and needs to be reviewed manually to filter out false detections. Attempts at extracting information about eruption kinematics automatically also failed. Nevertheless, we find it an useful tool for preliminary selection of events visible in SDO/AIA data.

Acknowledgements

We acknowledge financial support from the Polish National Science Centre grant number 2011/03/B/ST9/00104.

References

Amari, T. & Luciani, J. F. 1999, *ApJL*, 515, L81
&Archontis, V. and Török, T. 2008, *A&A*, 492, L35
Gilbert, H. R., Alexander, D., & Liu, R. 2007, *Sol. Phys.*, 245, 287
Hurlburt, N., Cheung, M., & Schrijver, C., *et al.* 2012, *Sol. Phys.*, 275, 67-78
Hurlburt, N. 2015, *arXiv preprint*, 1504.03395
Ji, H., Wang, H., Schmahl, E. J., Moon, Y.-J., & Jiang, Y. 2003, *ApJL*, 595, L135
Kushwaha, U., Joshi, B., Veronig, A. M., & Moon, Y.-J. 2015, *arXiv preprint*, 1504.01888
Mrozek, T. 2011, *Sol. Phys.*, 270, 191
Netzel, A., Mrozek, T., Kołomański, S., & Gburek, S. 2012, *A&A*, 548, A89
Song, H. Q., Zhang, Jie., & Cheng, Xin., *et al.* 2014, *ApJ*, 784, 48
Török, T. & Kliem, B. 2005, *ApJL*, 630, L97
Vršnak, B. 1990, *Sol. Phys.*, 129, 295
&Wang, Y. and Zhang, J. 2007, *ApJ*, 665, 1428